Int. J. Electrochem. Sci., 6 **(2011)** 5146 - 5160

International Journal of
ELECTROCHEMICAL
SCIENCE
www.electrochemsci.org

Sandwich-Type Electrochemiluminescence Immunosensor Based on PDDA-G@Lu-Au Composite for Alpha-Fetoprotein Detection

Ning Gan[1,*], *Jianguo Hou*[1,$], *Futao Hu*[1], *Yuting Cao*[1], *Tianhua Li*[1], *Lei Zheng*[2,*], *Jun Wang*[1]

[1] Faculty of Materials Science and Chemical Engineering, Ningbo University, 315211, China
[2] Nangfang Medical Hospital, Guangzhou, 41000, China
[$] Co-first author
[*]E-mail: ganning@nbu.edu.cn

Received: 14 September 2011 / *Accepted:* 16 October 2011 / *Published:* 1 November 2011

An ultrasensitive multiplexed electrochemiluminescence immunoassay method was developed for the detection of tumor markers by combining a functionalized graphene nanosheets and gold-coated magnetic Fe_3O_4 nanoparticles (GMPs) labeled alpha-fetoprotein (AFP) antibody (GMP~Ab1). The functionalized graphene nanosheets (PDDA-G) with poly (diallyldimethylammonium chloride) (PDDA) were synthesized and used to combine with luminol-capped gold nanoparticles (Lu-Au NPs). The resulting PDDA-G@Lu-Au composite displayed an enhanced capability for the immobilization of horseradish peroxidase (HRP) and signal antibody (Ab2) to realize its electrochemiluminescence immunoassay. Great signal amplification was achieved since PDDA-G could adsorb large amount of reporter molecules (Lu-Au). Besides gold nanoparticles were not only used as carriers of Ab2 and HRP but also catalyzed the ECL reaction of luminol, which further amplified the ECL signal of luminol in the presence of H_2O_2. GMPs as supporting material, not only been performed the rapid separation and purification of signal antibody on magnetic field, but also enhanced the fixed capacity of Ab1 to improve detection range. In addition, the magnetic probes were readily immobilized on the working electrode of screen-printed carbon electrode (SPCEs) by magnets. Under the optimized conditions, the ECL method shows a linear range of alpha-fetoprotein (AFP) from 0.002 to 20 ng mL^{-1} and an extremely low detection limit of 0.2 pg mL^{-1} (3σ). Moreover, the proposed method is also simple, stable, specific, and time-saving, avoiding the complicated process modification on the electrodes' surface, which may open a new door to ultrasensitive detection of tumor markers in clinical analysis.

Keywords: Alpha-fetoprotein, Gold-coated magnetic Fe_3O_4 nanoparticles (GMPs), Screen printed carbon electrode, PDDA functionalized grapheme (PDDA-G).

1. INTRODUCTION

The increasing demands of cancers diagnostics and therapeutic analysis require the development of sensitive and accurate detection of tumor markers. The immunoassay, based on the highly specific antibody–antigen recognition, has been widely used in the sensitive quantitative detection of tumor markers [1-6]. In comparison to the conventional immunoassays such as enzyme-linked immunosorbent assay (ELISA) and chemiluminescence immunoassay, the ECL assay not only shows high sensitivity and wide dynamic concentration response range but also is potential and spatial controlled. By integrating the high affinity of antigen-antibody, the ECL immunoassay has become a powerful analytical tool for highly sensitive and specific detection of clinical samples [7-9]. ECL immunosensors provide a disposable, sensitive and selective method for determining target proteins with shortened assay time and simplified operations [10].

However, the sensitivity of the ECL immunoassay is still low. In order to meet the increasing demand for early and ultrasensitive detection of biomarkers, various signal amplification technologies using nanomaterials have been developed. Since the nanoparticles can work as a promoter to increase the surface area and improve the electron transfer at the electrode interface. They can also be used as carriers to load a large amount of ECL labels and biomolecules and thus afford substantial ECL signal amplification and the enhancement of performances of the biosensors. Varieties of nanoparticles, such as gold nanoparticles (Au NPs), carbon nanotube, TiO_2 and SiO_2, have been applied as the labels in nanoparticle-based amplification platforms which can dramatically enhance the signal intensity of ECL immunosensors [11-16]. For example, Cui's group gained a great enhancement on the sensitivity of the ECL immunosensor using luminol-conjugated gold nanoparticles [17]. Yuan's group achieved enhanced sensitivity using a single-wall carbon nanotube forest modified electrode with silica nanoparticles loaded with $Ru(bpy)_3^{2+}$ and secondary antibody for the ECL immunoassay of Immunoglobulin G (IgG) [18].

The interesting physical properties of graphene, a novel one-atomthick and two-dimensional graphitic carbon system, has recently attracted enormous attention in constructing electrochemical biosensors [19-24]. Since the large surface area of graphene and related derivates also allows it to be an excellent carrier to load more active probes and active domains for biomolecules binding, offering a significant amplification on the electrochemical sensing signals. For example, the polyethylenimine-functionalized graphene ionic liquid nanocomposites, the conductive architecture of the graphene-doped chitosan complex and the positive poly (diallyldimethylammonium chloride) (PDDA) functionalized grapheme (PDDA-G) can possibly be used for the future fabrication of biosensors due to their good electronic properties and the biocompatibility of graphene-based composites produced by direct electron transfer in the biomolecule as it maintains bioactivity [25-27].

The magnetic nanoprobes strategy developed recently has proven to be a highly sensitive technique for detecting human tumor cells, and is especially well suited to separate and in the meantime detect low-concentrations of proteins [28, 29]. Besides using GMPs as a matrix to immobilize bimolecular has aroused great interests in recent years [30-34]. Qiu's group has reported that the dopamine biosensor was fabricated by immobilizing of ferrocenylalkanethiol molecules on the surface of Au-coated magnetic NPs and used to determine dopamine [33]. Pham's group has reported

that magnetic separation of biological molecules using Au-coated magnetic oxide composite NPs was examined after attachment of protein immunoglobulin (IgG) through electrostatic interactions [34]. Therefore, the GMP composite nanoparticles can be used not only to immobilize AFP antibody (anti-AFP) but also to prepare "magnetic graphene" probes. More importantly, the magnetic probes can be modified or removed from the surface of SPCEs in magnetic field. All these steps can make the electrode's surface renewable and simplified the electrode's modification steps.

In this paper, we have developed a novel and simple ECL immunosensor based on the highly intense ECL of PDDA-G@Lu-Au coupled with excellent biocompatibility and stability of GMPs labeled first antibody (anti-AFP~GMP). In this study, GMPs as supporting material, not only perform the rapid separation and purification of signal antibody on magnetic field, but also enhances the fixed capacity of Ab1 to improve detection range. Furthermore, the magnetic probes were readily immobilized on the working electrode of SPCEs by magnets, therefore, the electrode do not require complex modification and cleaning as traditional electrochemical immunesensors. In addition, the PDDA-G@Lu-Au composites exhibited dual amplification since PDDA-G could adsorb large amount of reporter molecules (Lu-Au) and gold particles could provide large active surface to load more HRP. Thus the GMPs~Ab1/AFP/HRP-Ab2~Au-Lu@PDDA-G magnetic probes were easy to control and have strong ECL signal. The experimental results indicated that the immunosensor exhibited good performance for detection of AFP with a wide linear range and a low detection limit.

2. EXPERIMENTAL PART

2.1. Reagents and Materials

Alpha-fetoprotein antibody (Anti-AFP, 1 mg mL^{-1}) was from Biocell Company (Zhengzhou, China). Luminol, Horseradish peroxidase (HRP EC 1.11.1.7, RZ>3.0, A>250 U/mg) and PDDA (MW: 100,000–200,000 $g \cdot mol^{-1}$, in 20% aqueous solution) were purchased from Sigma Co. Ltd. Hydrogen tetrachloroaurate (III) tetrahydrate ($HAuCl_4 \cdot 4H_2O$) and BSA (96~99%) were bought from Sinopharm Group Chem. Re. Co., Ltd. (Shanghai, China). Phosphate buffered solution (PBS, pH 7.4) was prepared using 0.1 M Na_2HPO_4, 0.1 M KH_2PO_4 and 0.1 M KCl. Blocking buffer solution consisted of a PBS with 3% (w/v) BSA and 0.05% (v/v) Tween 20. Washing buffer solution consisted of a PBS with 0.1 M NaCl and 0.05% (v/v) Tween 20 (PBST).

All other chemicals were of analytical grade and all solutions were prepared with doubly distilled water.

2.2. Apparatus

ECL experiments were carried out using a MPI-B model electrochemiluminescence analyzer (Xi'an Remax Electronic Science &Technology Co. Ltd., Xi'an, China) with the voltage of the photomultiplier tube being set at 800 V. The Transmission electron microscope (TEM) images were obtained using a HITACHI H-7650 (Hitachi, Japan). UV-Vis images were carried out using a TU-

1901UV-Vis spectrometer from Beijing Purkinje General Instrument Co. (Beijing, China). The X-ray powder diffraction (XRD) images were obtained using a Bruker D8 Advance diffractometer (Bruker, Germany). SPCEs (4 mm diameter) were purchased from DropSens Corporation (Spain), which consists of a carbon working electrode, a carbon auxiliary electrode and an Ag/AgCl reference electrode.

2.3. Preparation of GMP~Ab1

The synthesis of Fe_3O_4 magnetic NPs was achieved in a typical procedure according to reference [35]. Core–shell Fe_3O_4@Au NPs (GMPs) were prepared by growing Au layers onto the surface of the Fe_3O_4 as described by Williams [36]. The GMPs were obtained and dispersed in distilled water to a final volume of 10 mL. 1.0 mL GMPs solution was initially adjusted to pH 8.2 using Na_2CO_3, and then 1.0 mL of the original anti-AFP was added into the mixture and incubated for 24 h at 4 °C with slightly stirring. After magnetic separation, the obtained GMP~Ab1 bioconjugates were incubated with 3.0% BSA for 1 h to block the unreacted and nonspecific sites. The synthesized GMP~Ab1 bioconjugations were stored in 2 mL of pH 7.4 PBS at 4 °C when not in use. The final product obtained was shown in scheme 1.

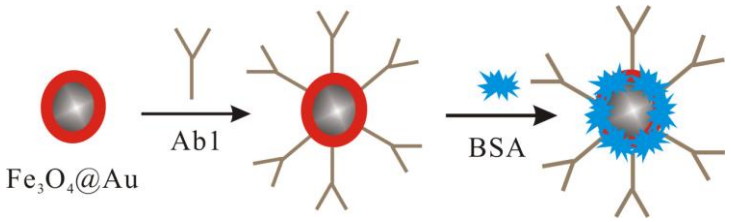

Scheme 1. Schematic illustration of the preparing procedures of GMP~anti-AFP probes

2.4. Preparation of PDDA-G@ Lu -Au ~HRP-Ab2

Luminol functionalized Au NPs (Lu-Au) with a diameter of 20 nm were prepared by reducing $AuCl_4^-$ ions with 0.01 mol L^{-1} luminol and stored at 4 ^oC, according to reference [37]. The unreacted reagents were removed via dialysis for 2 days with distilled water about six times under stirring by use of a 3500 molecular weight cut-off dialysis membrane to obtain Lu-Au NPs.

Graphene Oxide (GO) dispersion was prepared from graphite according to a modified Hummer's method [38] and its concentration was estimated by calibration curve from the absorbance at 231 nm in the UV–Vis spectra. PDDA-G was prepared according to Liu's method [27] and redispersed in water with a final concentration of 1.0 mg mL^{-1}. Then, 4 mL of the as-prepared PDDA-G dispersion was added into 20 mL Lu-Au NPs solution and sonicated for 30 min. After centrifugation, the colorless supernatant was casted and the obtained PDDA-G@Lu-Au composites were further washed with water for three times and redispersed in 8 mL water for further use.

50 μL Ab2 (10 μg mL^{-1}) and 100 μg HRP were added to 1.0 mL above PDDA-G@Lu-Au composite solution and shaken 24 h at 4 ^{o}C. After centrifuged at 20,000 rpm, the obtained bioconjugates (PDDA-G@Lu-Au~HRP-Ab2) were blocked with 3% BSA for 1 h at 4 ^{o}C, and then washed with PBS (pH 7.4) solution for at least three times, resuspended in 1.0 mL PBS (pH 7.4) that contained 0.1% BSA solution and stored at 4 °C for further work. The procedure was shown in Scheme 2.

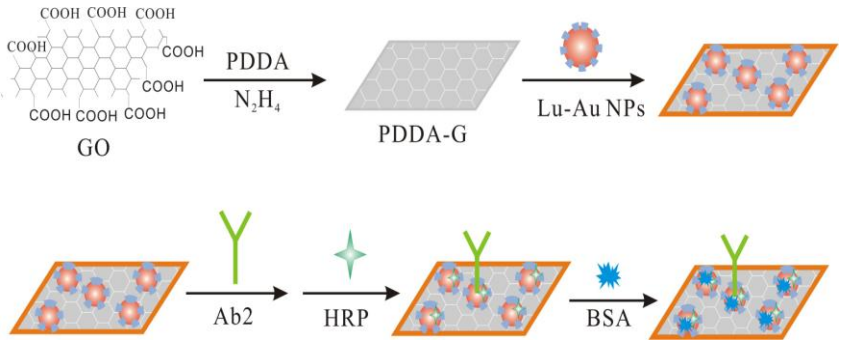

Scheme 2. Schematic illustration of the preparing procedures of PDDA-G@Lu-Au~HRP-Ab2

2.5. Preparation of the magnetic sandwich-type immunocomplexes

The schematic of the fabrication process was shown in Scheme 3. The immunocomplexes were prepared as follows: a mixture of 50 μL Fe_3O_4@ Au, 50 μL different concentrations of AFP and 50 μL RuL-MWNTs@Au~RuL-Ab2 was prepared and placed for 20 min at room temperature. After that, the PDDA-G@Lu-Au~HRP-Ab2/AFP/Ab1~GMP sandwich-type immunocomplexes were obtained by magnet, washed with PBST solution three times, dispersed in 50 μL PBS (pH 7.4) and stored at 4 °C for ECL tests.

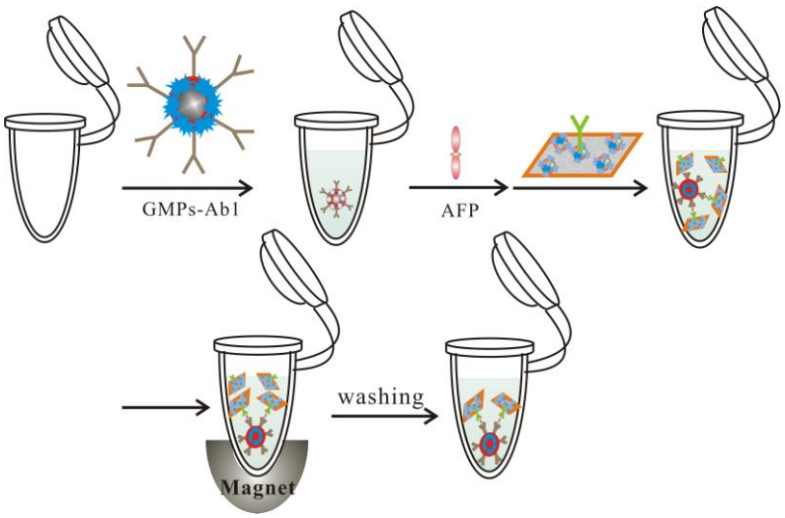

Scheme 3. The preparing procedures of the magnetic sandwich-type immunocomplexes.

2.6. ECL Measurements

The immunoassay procedure was illustrated in Scheme 4. For each test, 5 μL magnetic sandwich-type immunocomplex solution prepared with different concentrations of target AFP was attached on the cleaned SPCE surface with an NdFeB permanent magnet, ECL measurements were then performed in 35 μL CBS (pH 9.8) containing 2.0 mM H_2O_2 with a photomultiplier tube voltage of 800 V.

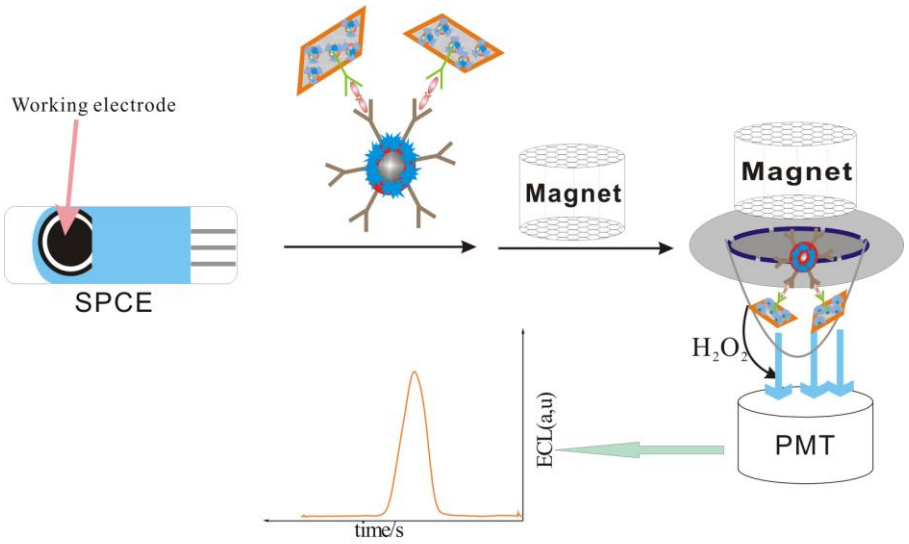

Scheme 4. The process of ECL measurements.

3. RESULTS AND DISCUSSION

3.1. Characterization of GMPs~Ab1 and PDDA-G@Lu-Au~HRP-Ab2 immunecomplexes

In this work, the GMPs were used to label anti-AFP (Ab1) because its high specific surface area may enhance the immobilized capacity toward Ab1. And PDDA-G matrix loaded with Lu-Au NPs, named PDDA-G@Lu-Au, was prepared as ECL signal amplification labels and immobilization substrates for HRP and AFP signal antibody (Ab2).

TEM images showed that both Fe_3O_4 and GMPs were of well spherical structure and preferable monodisperisity in size. The average diameter of Fe_3O_4 nanoparticles and GMPs were about 20 nm (Fig. 1-a) and 40 nm (Fig. 1-b), respectively. Upon deposition of gold shell to the Fe_3O_4 nanoparticles, the diameters of the particles increased by about 20 nm, demonstrating that the Au shell was about 20 nm thick. And PDDA-G and PDDA-G@Lu-Au membrane also were characterized using TEM. As can be seen, an obvious difference could be discerned between the microstructures of PDDA-G (Fig. 1-c) and PDDA-G@ Lu-Au (Fig. 1-d), demonstrates that some individual Lu-Au NPs (~20 nm diameter) and cluster-shape Lu-Au NPs were successfully assembled on the surface of PDDA-G nanosheets.

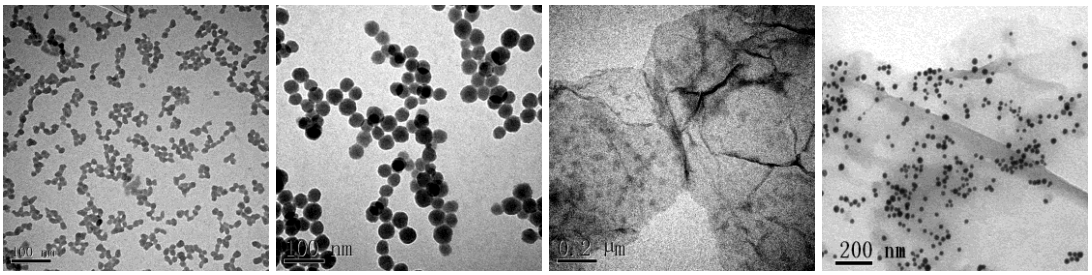

Figure 1. TEM images of (a) Fe_3O_4; (b) GMP; (c) PDDA-G; (d) PDDA-G@Lu-Au

In Figure 2A, the XRD spectra for Fe_3O_4, Au, and Fe_3O_4@Au nanoparticles were compared. The data (curve b) showed diffraction peaks at 2θ) 38.2°, 44.4°, 64.6°, 77.5°, and 81.7°, which can be indexed to (111), (200), (220), (311), and (222) planes of gold in a cubic phase, respectively (JCPDS no. 04-0784). Clearly, the XRD peaks for Fe_3O_4@Au nanoparticles (curve A-c) were similar to that for Au nanoparticles (curve A-b), but different from that for Fe_3O_4 nanoparticles (curve A-a). The absence of any diffraction peaks for magnetite was most likely due to the heavy atom effect from gold [39] as a result of the formation of Au-coated Fe_3O_4 nanoparticles. The fact provided strong evidence for complete coverage of the oxide core by Au supporting our TEM data, which supported the formation of Fe_3O_4@Au core-shell nanoparticles. And (Fig. 2B) showed that the GO (curve B-a) had a peak centered at 10.0°, while the reduction with hydrazine, no obvious peak was observed in PDDA-G (curve B-b), indicating the completely reduction of GO. After PDDA-G assembled with Lu-Au NPs, obvious peaks of Au NPs were observed (curve B-c), indicating the Lu-Au NPs assembled on the surface of PDDA-G, which was in accordance with TEM data.

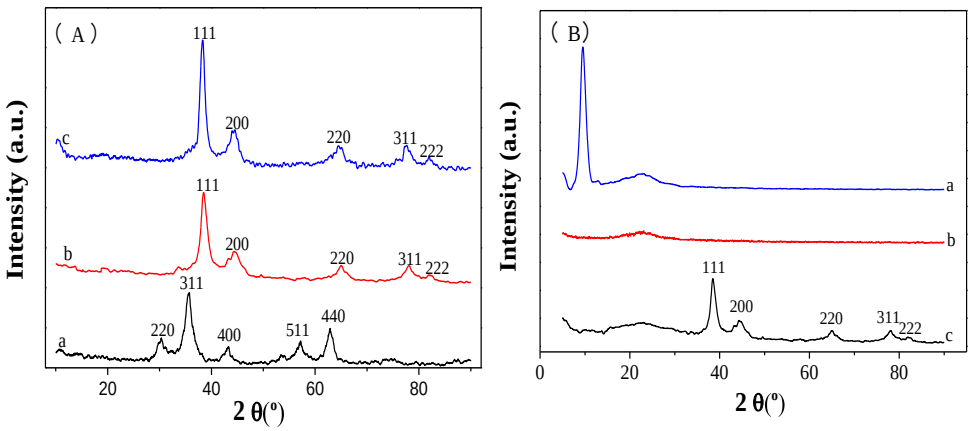

Figure 2. XRD images of A: a, Fe_3O_4 NPs; b, Au NPs; c, GMPs. B: a, GO; b, PDDA-G; c, PDDA-G@Lu-Au.

Measurements of the surface plasmon (SP) resonance band of the nanoparticles provided an indirect piece of evidence supporting the formation of GMPs core-shell morphology. Figure 3A shows

a typical set of UV-vis spectra comparing Fe_3O_4 (curve A-a) and GMPs (curves A-c). In contrast to the largely silent feature in the visible region for Fe_3O_4 particles, GMPs show a clear SP band at 532 nm. This band showed a red-shift in comparison with pure Au nanoparticles (curve A-b, 520 nm), indicating that the core–shell Fe_3O_4@Au NPs were formed by the deposition precipitation method. In addition, the anti-AFP molecules being labeled onto the surface of the GMPs, two absorption peaks at 280 and 540 nm were observed (curve A-e). One peak originated in the synthesized GMPs, another derived from the absorption peak of anti-AFP proteins (curve A-d, 280 nm). On the basis of the above results, it can be concluded that GMPs~Ab1 conjugation was successfully prepared and could be used in the electrochemiluminescence ELISA.

In Figure 3B, the as-prepared luminol-capped gold nanoparticles (Lu-Au NPs) (curve B-b) appeared a strong characteristic absorption peak at 530 nm caused by surface plasmon resonance. PDDA-G (curve B-a) showed a strong absorption peak at 270 nm which referred to $\pi \rightarrow \pi^*$ transitions of aromatic C=C bond indicating the restoration of the π-conjugation network of the grapheme nanosheets. Meanwhile, the band of $n \rightarrow \pi^*$ transition of C=O at about 300 nm was disappeared hinting the complete reduction of EGO [40]. After the Lu-Au NPs were assembled, the characteristic peak of Lu-Au NPs was observed in PDDA-G@Lu-Au (curve B-c) at 534 nm which indicated the efficient adsorption of Lu-Au NPs onto the PDDA-G nanosheets surface. Furthermore, the anti-AFP and HRP molecules being labeled onto the surface of the PDDA-G@Lu-Au, Three absorption peaks at 280, 400 and 534 nm were observed (B-e), One peak originated in the synthesized PDDA-G@Lu-Au (534 nm), the others derived from the absorption peaks of HRP (curve B-d, 400 nm) and anti-AFP (280 nm). In addition, one absorption peak of PDDA-G@Lu-Au (270 nm) was disappeared since the absorption peaks at 270 nm and 280 nm overlapped.

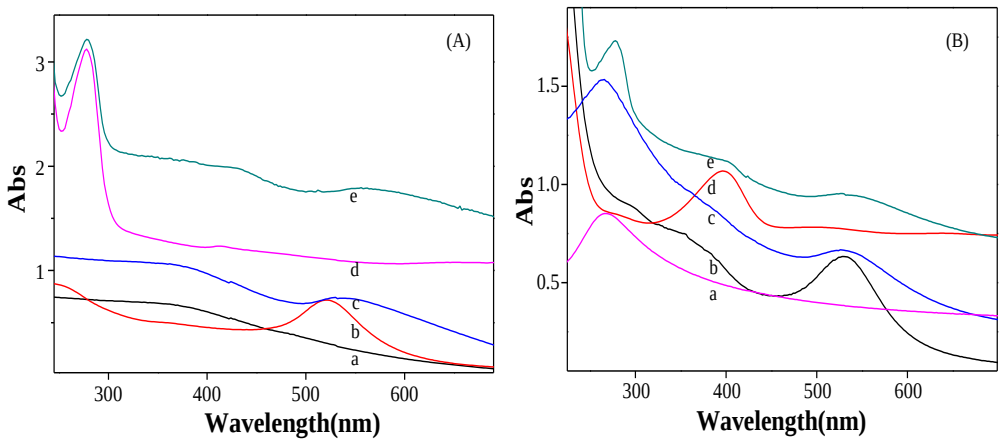

Figure 3. UV-Vis absorption spectra of A: a, Fe_3O_4 NPs; b, Au NPs; c, GMPs; d, anti-AFP (Ab1); e, GMPs~ Ab1 conjugation. B: a, PDDA-G; b, Lu-Au NPs; c, PDDA-G@Lu-Au; d, HRP; e, PDDA-G@Lu-Au~HRP-Ab2 conjugation.

3.2. ECL behavior of ECL immunosensor

The ECL behavior of the immunosensor was studied with a step potential in CBS containing 2.0 mM H_2O_2. To gain a better understanding of the ECL signal generation, Fig. 4a–d showed the ECL

signals of the bare SPCE, Ab1~GMPs/ SPCE, AFP/ Ab1~GMPs / SPCE, and PDDA-G@Lu-Au~HRP-Ab2/AFP/ Ab1~GMPs /SPCE, respectively. The results indicated that only the SPCE immobilized with PDDA-G@Lu-Au~HRP-Ab2 could produce ECL signals. Therefore, the ECL signals were from the PDDA-G@Lu-Au composites, which were due to the reaction of luminal radicals electro-oxidized by luminol with H_2O_2 under the catalysis of AuNPs and HRP [41, 42].

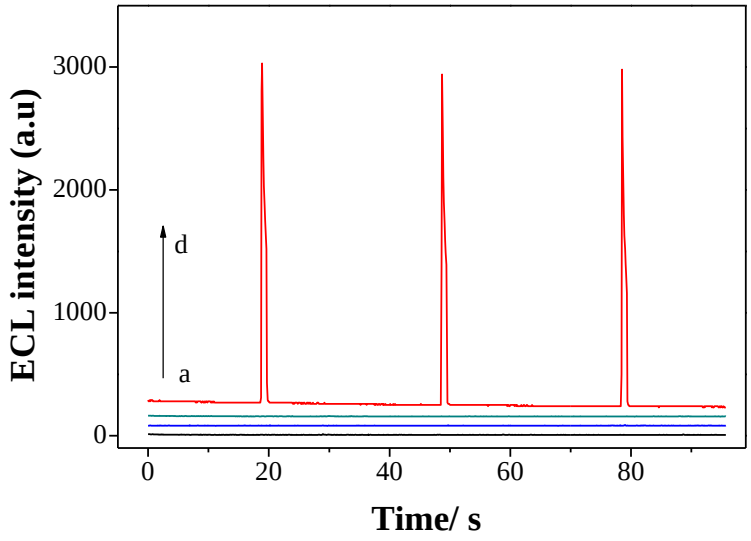

Figure 4. ECL signals under pulse potential obtained (a) on a bare SPCE, (b) on a AFP/Ab1~GMPs/SPCE, (c) on a AFP/Ab1~GMPs/SPCE, (d) on a PDDA-G@Lu-Au~HRP-Ab2/AFP/ Ab1~GMPs /SPCE. All ECL signals were measured in 0.02 mol L^{-1} CBS (pH 9.8) solution containing 2.0 mM H_2O_2.AFP, 1 ng mL^{-1}; initial potential, 0 V; pulse period, 30 s; final potential, 0.8 V.

3.3. Optimal conditions for ECL reaction

It is well known that the ECL performance of luminol and its derivatives greatly depends on pH of the solution. The effect of pH in the range of 8.6–11.2 (CBS, 0.02 mol L^{-1}) was examined. The maximal ECL intensity was obtained at pH 9.8 (Fig 5A). Therefore, pH 9.8 was used in the following experiments.

The change of ECL intensity with the concentration of H_2O_2 was shown in Figure 5B. From Figure 5B, it can be seen that the ECL intensity markedly enhanced after the addition of H_2O_2. The ECL intensity increased with the increase of the concentration of H_2O_2 and reached a maximum at 2.0 mM. This trend might be caused by of the co-oxidation function of H_2O_2. When the concentration of H_2O_2 was higher than 2.0 mM, the ECL intensity decreased. Therefore, 2.0 mM H_2O_2 was selected in the following experiments.

The immunoreaction time is an important parameter for the GMP~Ab1, AFP and the specific recognition of PDDA-G@Lu-Au~HRP-Ab2 in the tube. By increasing the immunoreaction time, the ECL signal increased and reached a plateau after 35 min (Fig 5C), indicating a tendency to complete immunoreaction in the tube. Therefore, the optimal immunoreaction time was 35 min.

The sensitivity of the proposed immunosensor is relied on the formation of the immunocomplex on the electrode which is dependent on the amount of HRP and Ab2 conjugated on the PDDA-G@Lu-Au. More HRP molecules on the PDDA-G@Lu-Au will enhance the ECL intensity. However, an excessive amount of HRP will also reduce the quantity of Ab2 and weaken the binding between PDDA-G@Lu-Au, AFP and GMP~Ab1. To obtain the best performance of the immunosensor, PDDA-G@Lu-Au modified with HRP and Ab2 at different mass ratios were synthesized and used for the construction of the immunocomplex (Fig 5D). As shown, the maximal ECL signal was achieved at a mass ratio of HRP to Ab2 of 200. Thus, the functionalized PDDA-G@Lu-Au synthesized in the solution with a mass ratio of HRP to Ab2 of 200 was employed in the modification of PDDA-G@Lu-Au for the following immunosensors construction.

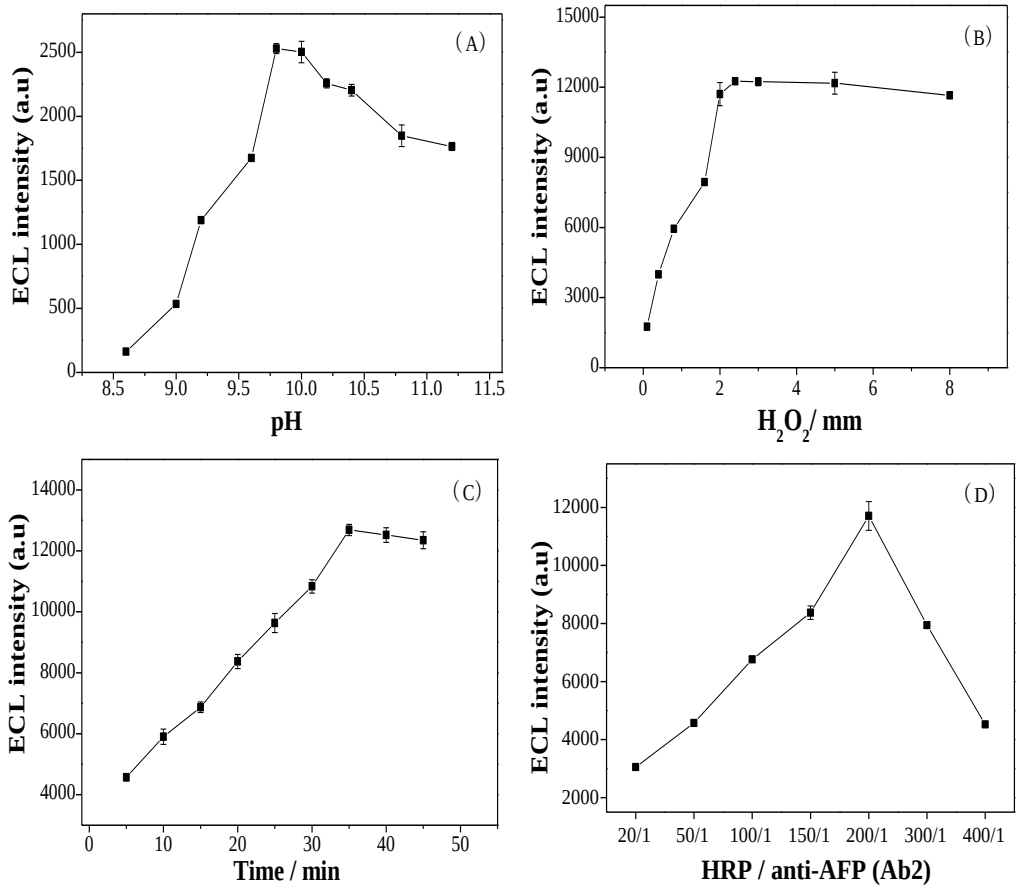

Figure 5. Effects of A) pH, B) H_2O_2 concentration, C) immunoreaction time, and D) HRP/anti-AFP (Ab2) ratio on ECL intensity. All ECL signals were measured in 0.02 mol L^{-1} CBS (pH 9.8) solution containing 2.0 mM H_2O_2; AFP, 10 ng mL^{-1}; initial potential, 0 V; pulse period, 30 s; final potential, 0.8 V.

3.4. Performance of the ECL immunosensor

Under selected conditions, the highly sensitive label of the magnetic sandwich-type immunocomplexes was then used to construct ECL immunosensors for AFP detection. The magnetic

sandwich-type immunocomplexes named PDDA-G@Lu-Au~HRP-Ab2/AFP/Ab1~GMPs were formed through antigen-antibody interaction in the presence of different concentrations of AFP. Then they were attached on SCPEs by magnet for ECL measurements. As the amount of PDDA-G@Lu-Au~HRP-Ab2/AFP/Ab1~GMPs sandwich-type immunocomplexes immobilized on the SCPEs was determined by the concentration of AFP, the ECL intensity (EI) of immobilized luminol in the presence of H_2O_2 could provide a sensitive output signal for AFP quantitative detection.

As shown in Figure 6, EI increased with the increasing of AFP concentration ranging from 0.002 to 20 ng mL^{-1}. A linear relation between the ΔEI and the logarithm of AFP concentration was obtained ΔEI = 8174.8 + 2925.3[Log (c_{AFP}/ng·mL^{-1})] with a correlation coefficient R = 0.9956. The detection limit was 0.2 pg·mL^{-1} (3σ). In order to make a comparison, the PDDA-G@Lu-Au~Ab2/AFP/ Ab1~GMPs (Figure 6B-b) and Lu-Au~Ab2/AFP/Ab1~GMPs (Figure 6B-c) sandwich-type immunocomplexes modified electrodes without HRP or PDDA-G were also evaluated, respectively. Compared with the proposed immunosensor (Figure 6B-a), a lower ECL response was observed.

To further highlight the advantages of the ECL immunosensors, the analytical properties of the developed immunoassay were compared with those of other AFP immunosensors reported previously. As shown in Table 1, it is obvious that the LOD of our sensor was lower than others. The results indicated that with the large surface area of PDDA-G, more amount of signal molecules (luminal) were immobilized on the proposed immunosensor. And the large amount of HRP absorbed onto the Au-NPs surface also enhanced the ECL signal. Thus the proposed ECL immunosensor based on the PDDA-G@Lu-Au~HRP-Ab2 immunocomplexes can greatly improve the detection sensitivity.

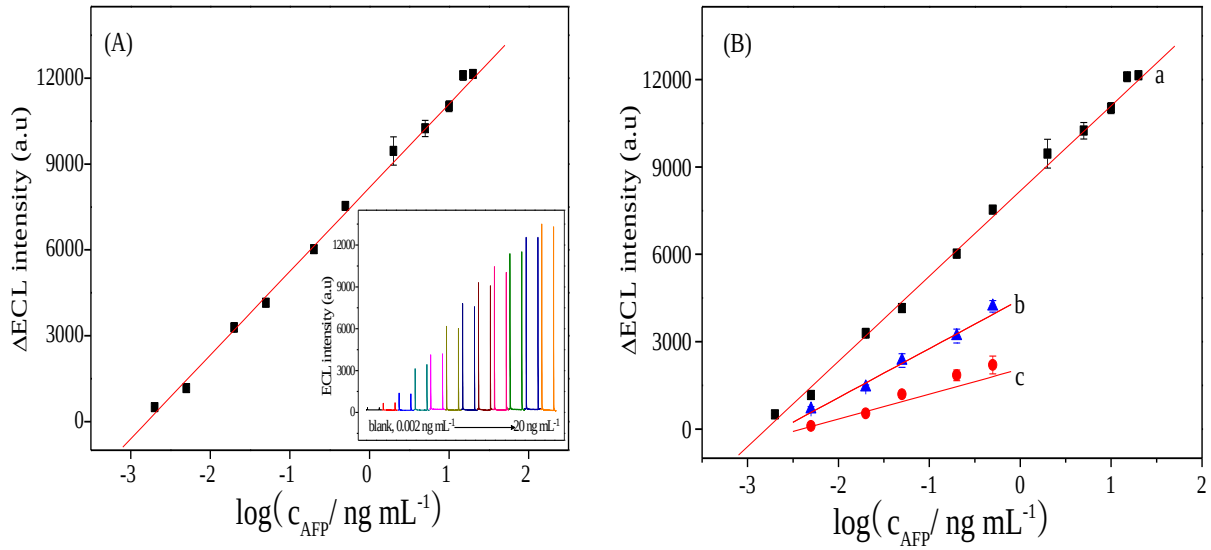

Figure.6. A) The schematic illustration of the ECL profiles of the immunosensor before (0.00 ng mL^{-1}) and after (0.002 ng mL^{-1}-20 ng mL^{-1}) incubating in different concentration of AFP. Insert: the relationship between ECL signals towards log of different AFP concentrations. B) The calibration curve of the immunosensor modified with PDDA-G@Lu-Au~HRP-Ab2 (a); PDDA-G@Lu-Au~ Ab2 (b) and Lu-Au~ Ab2 (c) immunocomplexes.

Table 1. Comparison of analytical properties of various AFP immunosensors and immunoassays.

Assay method	Detection antibody	LOD (/ng mL^{-1})	Ref.
Electrochemistry ELISA	PB@HAP~HRP-anti-AFP	0.009	[43]
	Carbon nanospheres~HRP-anti-AFP	0.02	[44]
Voltammetric ELISA	HRP-anti-AFP	3.7	[45]
Chemiluminescence	HRP-anti-AFP	0.23	[46]
Photoelectrochemistry	Label-free	0.04	[47]
Electrochemiluninescence	Ru-silica@Au~anti-AFP	0.03	[12]
	PDDA-G@Lu-Au~HRP-anti-AFP	2.0×10^{-4}	This work

3.5 Specificity for the detection of AFP

To investigate the selectivity and validate the sensor performance for AFP detection, the proposed immunosensor was tested using human plasma as matrix. The immunosensor was incubated in human plasma samples spiked with 10.0 ng mL^{-1} AFP and different possible interfering agents such as CEA, HIgG, BSA, HCG, DA and CA19-9. No remarkable ECL response change was observedfor the mixed sample in comparison to the result obtained only in the presence of AFP (Fig .7), indicating good selectivity for determination of AFP.

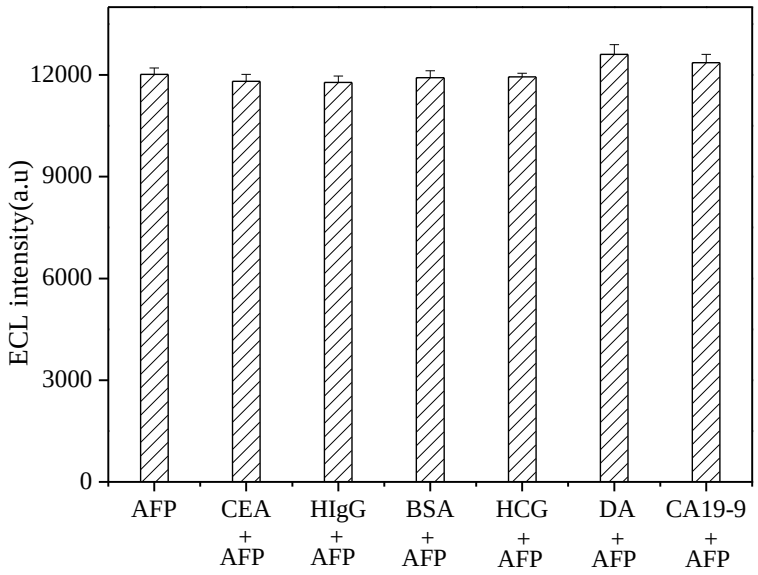

Figure 7. Selectivity analysis of the ECL immunosensor in the presence of different interferents. The concentrations of the interferents were: CEA (10 ng mL^{-1}), HIgG (10 ng mL^{-1}), BSA (1 μg mL^{-1}), HCG (10 ng mL^{-1}), DA (1 μg·mL^{-1}), CA19-9 (10 ng mL^{-1}). All ECL signals were measured

in 0.02 mol L^{-1} CBS (pH 9.8) solution containing 2.0 mM H_2O_2; initial potential, 0 V; pulse period, 30 s; final potential, 0.8 V.

3.6. Determination of AFP in human serum samples

Table 2. The recovery of the proposed immunosensor in human serum.

Sample number	Added (/ng mL^{-1})	Found (/ng mL^{-1})	Recovery (/ %)
1	0.050	0.053±0.003	106.0
2	0.50	0.46±0.02	92.0
3	2.00	2.12±0.20	106.0
4	5.00	4.82±0.30	96.4
5	10.0	10.27±0.38	102.7

[1]Mean value ± SD of three measurements

In order to investigate the possible application of this immunosensor in clinical analysis, recovery experiments were performed by standard addition methods in human serum. The experimental results were shown in Table 2 and the recovery was in the range from 92.0% to 106.0%, which indicated that the developed sensor might be applied for the determination of AFP in human serum for routine clinical diagnosis.

3.7. The stability of PDDA-G@Lu-Au~HRP-Ab2 and GMPs~Ab1 immunecomplexes

On the other hand, the stability of the PDDA-G@Lu-Au~HRP-Ab2 and GMPs~Ab1 immunecomplexes was tested. In order to do that, different centrifuge tubes containing the same amount of conjugates were prepared on the same day and stored in a refrigerator at 4 ◦C. Thereafter, each conjugate was used to measure the analytical signal for 10 ng mL^{-1} AFP during a period of time of 35 days. The RSD value obtained (n = 6) was 5.6% which demonstrated excellent stability of the PDDA-G@Lu-Au~HRP-Ab2 and GMPs~Ab1 conjugates for at least 35 days provided they were stored in refrigerator at 4 ◦C.

4. CONCLUSIONS

In this paper, one type of PDDA-G@Lu-Au probes was successfully prepared by a simple synthetic method. The obtained PDDA-G@Lu-Au composite particles could be an ideal substrate for antibody and HRP immobilization with high luminol capacity load efficiency, good stability and bioactivity. Furthermore, multilabel-antibody functionalized Fe_3O_4 (core)/Au (shell) composites were also prepared and applied as labels in sandwich electrochemiluminescence immunoassay. Due to the dual signal amplification strategy of PDDA-G-based particles and high luminol capacity of the probe, the electrochemiluminescence response of the fabricated immunosensor is greatly enhanced and

achieved the sensitive detection of AFP. Furthermore, the magnetic sandwich-type immunocomplexes can be modified and removed from its surface by magnetic field added on the flat bottom of SPCEs, The proposed electrochemiluminescence immunosensor is large since point-of-care analyses would reduce costs, minimize sample decomposition, facilitate on-the-spot diagnosis, and alleviate patient stress. Therefore, this novel dual amplified strategy opened a new door to broaden the potential applications of early diagnosis in cancer in clinical research.

ACKNOWLEDGMENTS
The authors appreciate the support of the National Natural Science Foundation of China (no. 20805024, 10874095) and Natural Science Foundation of Ningbo (2011A610018, 2011A610006), the Scientific Research Foundation of Graduate School of Ningbo University (YK2009045), the K.C.Wong magna fund in Ningbo University, Science and Technology Planning Project of Guangdong Province (No. 2010A030300006, No. 2008A050200006).

References

1. U. Bilitewski, *Anal. Chem.* 2000, *72*, 692A-701A.
2. J.M. Van Emon, V. Lopez-Avila, *Anal. Chem.* 1992, *64*, 79A-88A.
3. J. Wu, F. Yan, X.Q. Zhang, Y.T. Yan, J.H. Tang and H.X. Ju, *Clin. Chem.* 2008, *54*, 1481-1488.
4. W.L. Shelver, C.D. Parrotta, R Slawecki, Q.X. Li, M.G. Ikonomou, D. Barcelo, S. Lacorte, F.M. Rubio, *Chemosphere.* 2008, *73*, S18-S23.
5. D.P. Tang, R. Yuan, Y.Q. Chai, *Clin. Chem*. 2007, *53*, 1323-1329.
6. A.P. Deng, M. Himmelsbach, Q.Z. Zhu, S. Frey, M. Sengl, W. Buchberger, R. Niessner, D. Knopp, *Environ. Sci. Technol.* 2003, *37*, 3422-3429.
7. T. Ala-Kleme, P. Makinen, T. Ylinen, L. Vare, S. Kulmala, P. Ihalainen, Peltonen, J. *Anal. Chem*. 2006, *78*, 82-88.
8. X. Liu, H.X. Ju, *Anal. Chem.* 2008, *80*, 5377-5382.
9. W. Miao, A.J. Bard, *Anal. Chem.* 2004, *76*, 7109-7113.
10. H.Y. Wang, D.Y. Sun, Z.;Tan, W. Gong, L. Wang, *Colloids Surf. B: Biointerfaces.* 2011, *84*, 515-519.
11. J. Wang, *Small.* 2005, *1*, 1036-1043.
12. S.R. Yuan, R. Yuan, Y.Q. Chai, L. Mao, Yang, X. Y.L. Yuan, H. Niu, *Talanta*. 2010, *82*, 1468-1471.
13. Y. Tao, Z.J. Lin, X.M. Chen, X.L. Huang, M. Oyama, X. Chen, X.R. Wang, *Sens. and Act. B: Chem.* 2008, *129*, 758-763.
14. B. Haghighi, S. Bozorgzadeh, L. Gorton, *Sens. and Act. B: Chem.* 2011,*155*, 577-583.
15. L. Mao, R. Yuan, Y.Q. Chai, Y. Zhuo, X. Yang, *Sens. and Act. B: Chem.* 2010, *149*, 226-232.
16. J. Qian, Z.X. Zhou, X.D. Cao, S.Q. Liu, *Anal. Chim. Acta* 2010, *665*, 32-38.
17. D.Y. Tian, C.F. Duan, W. Wang, H. Cui, *Biosens. Bioelectron.* 2010, 25, 2290-2295.
18. X. Yang, R. Yuan, Y.Q. Chai, Y. Zhuo, L. Mao, S.R. Yuan, *Biosens. Bioelectron.* 2010, *25*, 1851-1855.
19. S. Virendra, J. Daeha, Z. Lei, D. Soumen *Prog. Mater Sci.* 2011, *56*, 1178-1271.
20. A.K. Geim, K.S. Novoselov, *Nat. Mater.* 2007, *6*, 183-191.
21. Y. Kopelevich, P. Esquinazi, *Adv. Mater.* 2007, *19*, 4559-4563.
22. D. Du, L.M. Wang, Y.Y. Shao, J. Wang, M.H. Engelhard and Y.H. Lin, *Anal. Chem.* 2011, *83*, 746-752.

23. Y. Wan, Y. Wang, J.J. Wu, and D. Zhang, *Anal. Chem.* 2011, *83*, 648-653.
24. Q. Wei, K.X. Mao, D. Wu, Y.X. Dai, J. Yang, B. Du, M.H. Yang, H. Li, *Sens. and Act. B: Chem.* 2010, *149*, 314-318.
25. C.S. Shan, H.F. Yang, J. F. Song, D.X. Han, A. Ivaska and L. Niu, *Anal. Chem.* 2009, *81*, 2378-2382.
26. S. Xu, Y. Liu, T. Wang, J. Li, *Anal. Chem.* 2011, *83*, 3817-3823.
27. K.P. Liu, J.J. Zhang, G.H. Yang, C.M. Wang, J.J. Zhu, *Electrochem. Commun.* 2010, *12*, 402-405.
28. J. Zhang, S. Song, L. Zhang, L. Wang, H. Wu, D. Pan, C. Fan, *J. Am. Chem. Soc*. 2006, *128*, 8575-8580.
29. A. Ambrosi, M.T. Castaneda, A.J. Killard, M.R. Smyth, S. Alegret, *Anal. Chem.* 2007, *79*, 5232-5240.
30. J.P. Li, H.L. Gao, Z.Q. Chen, X.P. Wei, C.F. Yang, *Anal. Chim. Acta* 2010, *665*, 98-104.
31. D.P. Tang, R. Yuan and Y.Q. Chai, *J. Phys. Chem. B.* 2006, *110*, 11640-11646.
32. H.N. Liu, S. Li, L.H. Liu, L. Tian, N.Y. He, *Biosens. Bioelectron*. 2010, *26*, 1442-1448.
33. J.D. Qiu, M. Xiong, R.P. Liang, H.P. Peng, F. Liu, *Biosens. Bioelectron*. 2009, *24*, 2649-2653.
34. T.T.H. Pham, C. Cao, S. J. Sim, *J. Magn. Magn. Mater.* 2008, *320*, 2049-2055.
35. Y.S. Kang, S. Risbud, J.F. Rabolt, P. Stroeve, *Chem. Mater.* 1996, *8*, 2209–2211.
36. J.L. Lyon, D.A. Fleming, M.B. Stone, P. Schiffer, M.E. Williams, *Nano Lett.* 2004, *4*, 719-723.
37. H. Cui, W. Wang, C.F. Duan, Y.P. Dong and J.Z. Guo, *Chem. Eur. J.* 2007, *13*, 6975-6984.
38. W.S. Hummers, R.E. Offeman, *J. Am. Chem. Soc.* 1958, *80*, 1339.
39. X.W. Teng, D. Black, N.J. Watkins, Y. Gao, H. Yang, *Nano Lett.* 2003, *3*, 261-264.
40. Y. Zhou, Q.L. Bao, L.A.L. Tang, Y.L. Zhong, K.P. Loh, *Chem. Mater.* 2009, *21*, 2950-2956.
41. Z.F. Zhang, H. Cui, C.Z. Lai, L.J. Liu, *Anal. Chem*. 2005, *77*, 3324-3329.
42. X.Y. Yang, Y.S. Guo, S. Bi, S.S. Zhang, *Biosens. Bioelectron*. 2009, *24*, 2707-2711.
43. Y.X. Dai, Y.Y. Cai, Y.F. Zhao, D. Wu, B. Liu, R. Li, M.H. Yang, Q. Wei, B. Du, H. Li, *Biosens. Bioelectron*. 2011, *28*, 112-116.
44. D. Du, Z.X. Zou, Y.S. Shin, J. Wang, H. Wu, M.H. Engelhard, J. Liu, I.A. Aksay, Y.H. Lin, *Anal. Chem.* 2010, *82*, 2989- 2995.
45. M. Giannetto, L. Elviri, M. Careri, A. Mangia, G. Mori, *Biosens. Bioelectron.* 2011, *26*, 2232-2236.
46. H. Huang, X.L. Zheng, J.S. Zheng, J. Pan, X.Y. Pu, *Biomed. Microdevices.* 2009, *11*, 213-216.
47. G.L. Wang, J.J. Xu, H.Y. Chen, S.Z. Fu, *Biosens. Bioelectron.* 2009, *25*,791-796.